# Maize resistance to witchweed through changes in strigolactone biosynthesis

Li, C.; Dong, L.; Durairaj, J.; Guan, J.C.; Yoshimura, M.; Quinodoz, P.; Horber, R.; Gaus, K.; Li, J.; Setotaw, Y.B.; Qi, J.; De Groote, H.; Wang, Y.; Thiombiano, B.; Floková, K.; Walmsley, A.; Charnikhova, T.V.; Chojnacka, A.; Correia de Lemos, S.; Ding, Y.; Skibbe, D.; Hermann, K.; Screpanti, C.; De Mesmaeker, A.; Schmelz, E.A.; Menkir, A.; Medema, M.; Van Dijk, A.D.J.; Wu, J.; Koch, K.E.; Bouwmeester, H.J.

**DOI**
10.1126/science.abq4775

**Publication date**
2023

**Document Version**
Final published version

**Published in**
Science

PLANT SCIENCE

# Maize resistance to witchweed through changes in strigolactone biosynthesis

C. Li[1], L. Dong[1]*, J. Durairaj[2]†, J.-C. Guan[3], M. Yoshimura[4,5,6], P. Quinodoz[5], R. Horber[5], K. Gaus[5], J. Li[7], Y. B. Setotaw[7], J. Qi[7], H. De Groote[8], Y. Wang[1], B. Thiombiano[1], K. Floková[1,9], A. Walmsley[1], T. V. Charnikhova[1], A. Chojnacka[1], S. Correia de Lemos[2,10], Y. Ding[11], D. Skibbe[12], K. Hermann[5], C. Screpanti[5], A. De Mesmaeker[5], E. A. Schmelz[11], A. Menkir[13], M. Medema[2], A. D. J. Van Dijk[2], J. Wu[7], K. E. Koch[3], H. J. Bouwmeester[1]*

Maize (*Zea mays*) is a major staple crop in Africa, where its yield and the livelihood of millions are compromised by the parasitic witchweed *Striga*. Germination of *Striga* is induced by strigolactones exuded from maize roots into the rhizosphere. In a maize germplasm collection, we identified two strigolactones, zealactol and zealactonoic acid, which stimulate less *Striga* germination than the major maize strigolactone, zealactone. We then showed that a single cytochrome P450, ZmCYP706C37, catalyzes a series of oxidative steps in the maize-strigolactone biosynthetic pathway. Reduction in activity of this enzyme and two others involved in the pathway, ZmMAX1b and ZmCLAMT1, can change strigolactone composition and reduce *Striga* germination and infection. These results offer prospects for breeding *Striga*-resistant maize.

Food security is a growing challenge in the face of climate change and increasing food needs (*1*). Maize (*Zea mays*) is one of the most important staple crops in the world, especially in Africa. There, its yield is compromised by the parasitic witchweeds *Striga hermonthica* and *Striga asiatica*. Damage from these *Striga* species threatens the livelihood of millions of people, particularly in sub-Saharan regions (fig. S1) (*2*, *3*). *Striga* seeds lay dormant in soil until their germination is triggered by strigolactones (SLs), signaling compounds exuded by the roots of plants, including maize. The first known SL, strigol, was discovered in the 1960s in the root exudates of cotton (*4*). In addition to having been co-opted as a cue for root-parasitic plants, SLs serve as host signals for beneficial arbuscular mycorrhizal fungi (AMF) and are plant hormones with developmental roles (*5*–*9*).

Thus far, more than 35 different SLs have been discovered, all containing the conserved D-ring (Fig. 1A) (*10*–*12*). The canonical SLs include two groups, the "strigol-type" and "orobanchol-type," whereas noncanonical SLs lack the A-, B-, and/or C-rings (*10*–*12*). Plants usually exude a blend of different SLs, and the composition of the root exudate can vary greatly between and sometimes also within plant species. Many of the SLs display substantial differences in their biological activity, such as the induction of AMF hyphal branching and parasitic plant germination (*9*, *13*–*15*). The biological importance of SL blends is far from understood, but in sorghum (*Sorghum bicolor*), a change in SLs from 5-deoxystrigol to orobanchol decreased *Striga* germination and increased field resistance (*16*).

The mechanisms of SL biosynthesis have only been partially elucidated. Three enzymes—DWARF 27 (D27) and two carotenoid cleavage dioxygenases 1(CCDs), CCD7 and CCD8—catalyze the conversion of β-carotene to carlactone (CL) (Fig. 1A) (*17*, *18*). In *Arabidopsis*, CL is oxidized to form carlactonoic acid (CLA) by a cytochrome P450 (CYP) monooxygenase, CYP711A1, encoded by More Axillary Growth 1 (MAX1) homolog AtMAX1 (*19*). *Arabidopsis* has a single copy of this MAX1, whereas maize has three homologs, and rice has five (*18*, *20*). Although both the *Arabidopsis* AtMAX1 and the maize ZmMAX1b form CLA from CL, the rice MAX1 homologs, Os900 and Os1400, instead convert CL to 4-deoxyorobanchol (4DO) and orobanchol, respectively (*18*, *21*). Dicots also form orobanchol, but from CLA rather than CL, and with a different cytochrome P450, CYP722C. A homolog of this CYP722C can also produce 5-deoxystrigol from CLA (*22*, *23*).

Maize roots exude at least six SLs, two of which have been structurally identified as zealactone and zeapyranolactone (Fig. 1A) (*24*–*26*). However, the identities of the other four SLs remained elusive, as well as the biosynthetic differences between the six and their individual roles in *Striga* germination. In this study, we reveal natural variation in the maize SL blend, identify three new maize SLs, elucidate the entire maize SL biosynthetic pathway, and show that changes in the composition of the SL blend correspond to differences in *Striga* germination and infection. These findings create a pathway for reducing the notorious agricultural problem of *Striga* infection through breeding maize for favorable SL composition.

### *Natural variation in strigolactone production by maize*

To assess the extent of variation in the production of SLs by maize, we grew a collection of maize genotypes, sampled their root exudate, and analyzed SLs with multiple reaction monitoring (MRM) liquid chromatography–tandem mass spectroscopy (LC/MS/MS) (Fig. 1B and figs. S2 and S3) (*24*, *25*). Quantities of exuded SLs varied among these lines (Fig. 1B and fig. S3). Moreover, one of the genotypes, NP2222, displayed a distinctive SL profile, lacking detectable levels of all but two SLs, an unknown SL and designated compound 5 (Fig. 1B and fig. S3). Compound 5 was previously noted in maize root exudate (*24*), but its low abundance and chemical instability hampered structural characterization. Therefore, on the basis of nuclear magnetic resonance (NMR) spectra and retrosynthetic analysis (*24*, *27*–*29*), we postulated structures and subsequently synthesized compound 5 as well as the other unknown SL (figs. S4 to S12). The synthetic products were identical to the natural ones in maize root exudate and were designated zealactol (compound 5) and zealactonoic acid (ZA) (the other unknown SL) (figs. S9 and S12). Bioassay of *Striga* germination showed that both zealactol and ZA were less inductive than zealactone (Fig. 1C), an outcome that highlights how strongly minute differences in SL structure can alter their biological activity. These findings are further supported by work on sorghum (*16*). To unravel the mechanistic basis for these differences in SL blends, we revealed the biosynthetic pathway of maize SLs.

### *Three maize genes encode the carlactone biosynthetic pathway*

Through homology, we identified the maize orthologs *D27*, *CCD7*, and *CCD8*, which catalyze the formation of CL from β-carotene in other plant species (tables S1 and S2). To confirm *ZmCCD8* function, we analyzed root exudate of two independent *zmccd8* mutants (in W22 and Mo17 backgrounds) (*30*). Zealactone was not detected, although it was the major SL in

[1]Plant Hormone Biology Group, Swammerdam Institute for Life Sciences, University of Amsterdam, Science Park 904, 1098 XH Amsterdam, Netherlands. [2]Bioinformatics Group, Wageningen University & Research, 6708 PB Wageningen, Netherlands. [3]Horticultural Sciences Department, University of Florida, Gainesville, FL 32611, USA. [4]Laboratorium für Organische Chemie, Department of Chemistry and Applied Biosciences, ETH Zürich, 8093 Zürich, Switzerland. [5]Syngenta Crop Protection AG, Schaffhauserstrasse 101, CH-4332 Stein, Switzerland. [6]Kyoto University, iCeMS, Yoshida Ushinomiya-cho, Sakyo-ku, Kyoto 606-8501, Japan. [7]Department of Economic Plants and Biotechnology, Yunnan Key Laboratory for Wild Plant Resources, Kunming Institute of Botany, Chinese Academy of Sciences, Kunming 650201, China. [8]International Maize and Wheat Improvement Center (CIMMYT), PO Box 1041-00621, Nairobi, Kenya. [9]Laboratory of Growth Regulators, Institute of Experimental Botany, The Czech Academy of Sciences and Faculty of Science, Palacký University, Šlechtitelů 27, 783 71 Olomouc, Czech Republic. [10]Plant genomics and transcriptomics group, Institute of Biosciences, Sao Paulo State University, 13506-900 Rio Claro, Brazil. [11]Section of Cell and Developmental Biology, University of California at San Diego; La Jolla, CA 92093, USA. [12]Seeds Research, Syngenta Crop Protection, LLC, Research Triangle Park, NC 27709, USA. [13]International Institute of Tropical Agriculture, PMB 5320 Oyo Road, Ibadan, Nigeria.
***Corresponding author. Email: h.j.bouwmeester@uva.nl (H.J.B.), l.dong2@uva.nl (L.D.)**
†Present address: Biozentrum, University of Basel, Spitalstrasse 41, 4056 Basel, Switzerland.

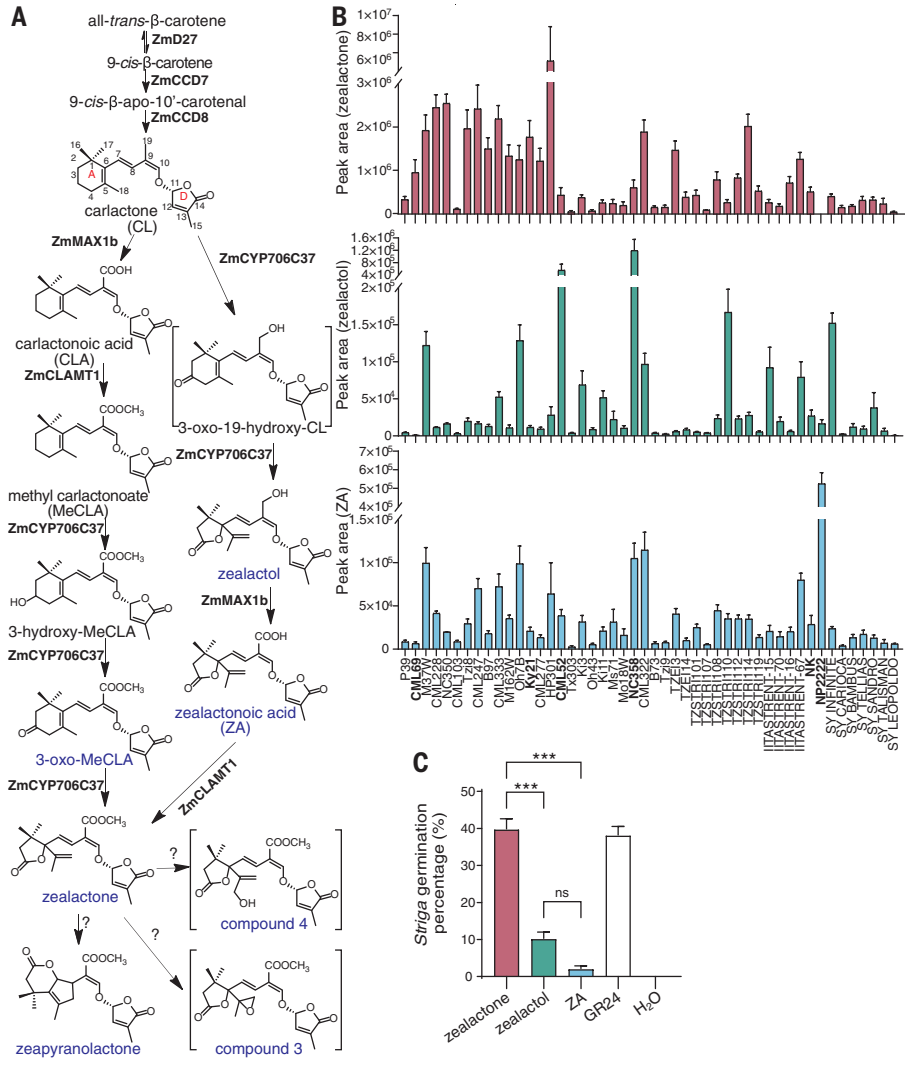


**Fig. 1. Discovery of two strigolactones with low *Striga* germination–inducing activity from maize line screening.** (**A**) Strigolactone (SL) biosynthetic pathway of maize. The enzymes identified in this study are shown in bold. SLs detected in maize root exudate are indicated in blue. Structures in square brackets are putative. (**B**) Detection of three maize SLs (zealactone, mass/charge ratio (*m/z*) 377 > 97; zealactol, *m/z* 331 > 97; ZA, *m/z* 363 > 249) in root exudate of a collection of maize lines. Names of lines selected for further analysis are indicated in bold. Data for the other four maize SLs are shown in fig. S3. (**C**) Induction of germination of *Striga* by zealactone, zealactol, and ZA (0.347 μM). GR24 (0.335 μM) and water were used as positive and negative control, respectively. Bars indicate means ± SEM. Ns, not significant ($P > 0.05$), ***$P < 0.001$, one-way ANOVA test followed by Tukey's multiple comparisons test comparing the mean of each column with the mean of every other column.

wild-type exudate (fig. S13A), showing that *ZmCCD8* is a key enzyme in maize SL biosynthesis (*17*, *31*, *32*). The transient expression of *ZmD27* (*GRMZM2G158175*), *ZmCCD7* (*GRMZM2G158657*), and *ZmCCD8* (*GRMZM2-G446858*) together in *Nicotiana benthamiana* led to accumulation of CL (Figs. 1A and 2A, fig. S14A, and table S3), which is consistent with results from rice and tomato orthologs (*21*, *33*).

### *Identification of gene candidates for carlactone conversion*

On the basis of the structures of the maize SLs identified thus far (Fig. 1A and fig. S2) (*24*–*26*), we postulated the involvement of a methyl transferase and several CYPs in the pathway downstream of CL. Several bioinformatic approaches were combined to select candidate genes for further functional characterization.

Mutual Rank (MR)–based global gene coexpression analysis (*34*, *35*) showed that of the three maize *MAX1* homologs, only *ZmMAX1b* tightly coexpressed with *ZmCCD8* (fig. S15), making it the strongest candidate for the next biosynthetic step. Analysis of root exudate from a *zmmax1a zmmax1c* double mutant (supplementary materials) showed wild-type levels of zealactone, thus excluding both homologs from being the biosynthetic genes we sought (fig. S13B). Earlier research also demonstrated that ZmMAX1b (GRMZM2G023952) converts CL to CLA more efficiently than does ZmMAX1a (GRMZM2G018612) or ZmMAX1c (GRMZM2G070508) (*18*). The amounts of CL in leaf extracts decreased after coinfiltration of *ZmMAX1b* with *ZmD27*, *ZmCCD7*, and *ZmCCD8* in *N. benthamiana*, (Fig. 2A), confirming that ZmMAX1b uses CL as a substrate (*18*). However, only traces of the expected product, CLA, were detected in this expression system (Fig. 2B and fig. S14B). To resolve this enigma, *N. benthamiana* extracts were analyzed with LC–quadrupole time-of-flight (QTOF)–MS. Prominent peaks of CLA-hexose and CLA-dihexose conjugates were detected in samples expressing the maize CL pathway genes together with *ZmMAX1b*. These conjugates were lacking in control samples and other gene combinations (Fig. 2C and table S4). Similar conjugation has been demonstrated for the transient production of other acidic compounds with *N. benthamiana* (*36*, *37*).

For selection of remaining candidate genes, we combined three approaches: (i) MR–based coexpression with *ZmCCD8* and *ZmMAX1b* as baits (fig. S15), (ii) coexpression modules in MaizeGGM2016 (*38*), and (iii) differential gene expression in a *zmccd8* mutant (Fig. 2D). For the latter, we assumed that SL pathway genes downstream of *CCD8* would be transcriptionally regulated in the *zmccd8* mutant (*33*). The *ZmCCD7*, *ZmCCD8*, and *ZmMAX1b* genes clustered together in MaizeGGM2016 module 091, suggesting that the 32 other genes in this module were candidates for the missing pathway genes (table S5). In the roots of *zmccd8* seedlings, 1301 genes were differentially expressed (DEGs) (less than or equal to twofold change, false discovery rate (FDR) < 0.05) compared with the B73 wild type (tables S5 and S6). These three approaches shared a seven-gene overlap (Fig. 2D and table S2) in which three [*GRMZM2G033126*, *GRMZM2G158342*, and *GRMZM2G023952* (*ZmMAX1b*)] formed a putative gene cluster on chromosome 3 (Fig. 2, D and E, and fig. S15) (*39*). Genes homologous to these also cluster in other *Poaceae* species (fig. S16), but the functional importance is unknown. So too is the identity of SLs produced by some of these species, such as switchgrass.

### *ZmCLAMT1 is a carlactonoic acid methyltransferase*

Because SLs zealactone and zeapyranolactone are methylesters, their proposed precursor has been methyl carlactonoate (MeCLA) (*24*). Thus, we sought a methyltransferase gene that causes the formation of MeCLA from CLA. We bioinformatically identified a top candidate (*GRMZM2G033126*) (Fig. 2, D and E), which

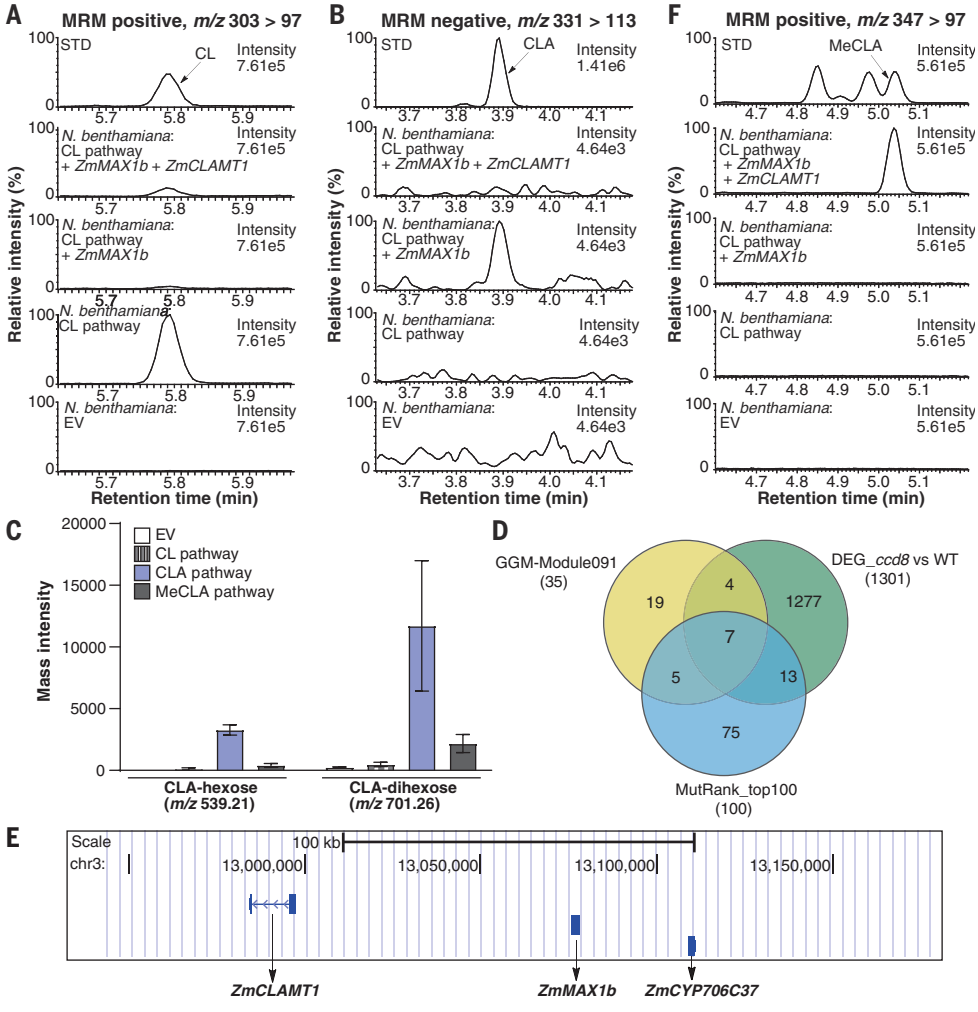


**Fig. 2. Identification of gene candidates for maize strigolactone biosynthesis.** (**A** and **B**) Representative MRM-LC/MS/MS chromatograms of carlactone (CL), $[M+H]^+$ *m/z* 303 > 97 (A), and carlactonoic acid (CLA), $[M-H]^-$ *m/z* 331 > 113 (B), in *N. benthamiana* leaf samples transiently expressing maize strigolactone (SL) precursor pathway genes. (**C**) Untargeted metabolomics to identify CLA conjugates in *N. benthamiana* leaf samples. *m/z* 539.21: CLA + hexose + formic acid − $H_2O$; *m/z* 701.26: CLA + 2 hexose + formic acid − $H_2O$ (**D**) Venn diagram of candidate gene numbers from several analyses: module091 from maizeGGM, genes differentially expressed in *zmccd8* roots (compared with wild type), and the top 100 genes coexpressed with *ZmCCD8* and *ZmMAX1b* (*34*, *35*). (**E**) Putative SL biosynthetic gene cluster on chromosome 3 consisting of *ZmCLAMT1*, *ZmMAX1b*, and *ZmCYP706C37*, adapted from screenshot from UCSC Genome Browser on *Z. mays* (B73 RefGen_v3) Assembly (zm3) (http://genome.ucsc.edu) (*39*). (**F**) Representative chromatograms of methylcarlactonoic acid (MeCLA), $[M+H]^+$ *m/z* 347 > 97, in *N. benthamiana* leaf samples. STD, standard; EV, empty vector infiltrated control sample. CL pathway, maize carlactone biosynthetic pathway genes, *ZmD27*, *ZmCCD7*, and *ZmCCD8*. CLA pathway, CL pathway genes + *ZmMAX1b*. MeCLA pathway, CLA pathway genes + *ZmCLAMT1*. Bars indicate mean ± SEM.

successfully produced MeCLA in *N. benthamiana* when transiently expressed together with genes for the maize CLA pathway (Fig. 2F). We therefore identified *GRMZM2G033126* as a carlactonoic acid methyltransferase gene and named the enzyme ZmCLAMT1 (Fig. 1A). The maize gene is an ortholog of *At4g36470*, which was recently found to encode a carlactonoic acid methyltransferase CLAMT in *Arabidopsis* (*40*, *41*).

### *ZmCYP706C37 catalyzes formation of several maize strigolactones*

The other candidate genes were coinfiltrated by different combinations of precursor-pathway genes. Coinfiltration of *ZmCYP706C37* (*GRMZM2G158342*) (*42*) by those encoding the MeCLA pathway decreased levels of MeCLA, indicating that this CYP can use MeCLA as a substrate (fig. S17A) and produce zealactone (Fig. 3A and fig. S2). To check for other possible biosynthetic pathways, we also coexpressed *ZmCYP706C37* with genes encoding the CL pathway enzymes. This combination resulted in production of zealactol (Fig. 4A and fig. S17B). Formation of both zealactone and zealactol involves complex rearrangement of the SL A ring and, for zealactol, a hydroxylation at C19 as well. To exclude the possibility of endogenous enzymes from *N. benthamiana* contributing to these complex conversions, we expressed *ZmCYP706C37* in yeast, isolated its microsomes, and analyzed product formation with different substrates (Figs. 3B and 4B). This approach confirmed that ZmCYP706C37 can convert MeCLA to zealactone and CL to zealactol (Fig. 1A).

To form zealactone from MeCLA, ZmCYP706C37 must catalyze several consecutive oxidative reactions with 3-hydroxy-MeCLA and 3-oxo-MeCLA as putative intermediates (Figs. 1A and 3C). The latter two compounds were previously synthesized as intermediates in the total synthesis of heliolactone (*43*). We used them here as substrates in our *ZmCYP706C37*-expressing yeast-microsome assay, and both were successfully converted to zealactone (Fig. 3D). We developed an MRM method for detection of these compounds (fig. S2) and identified them as intermediate products in the conversion of MeCLA to zealactone (fig. S18). Moreover, analysis of maize root exudate revealed that 3-oxo-MeCLA is also a natural maize SL previously referred to as compound 6 (fig. S19 and Fig. 1A) (*24*). These results demonstrate that a single enzyme, ZmCYP706C37, can catalyze the many oxidative steps necessary for the conversion of MeCLA to zealactone that were previously hypothesized to require several enzymes (Figs. 1A and 3C) (*24*).

For additional insight into the parallel biosynthetic pathway of CL to zealactol, we further analyzed samples from *N. benthamiana* and yeast microsome assays with untargeted metabolomics and MRM-LC-MS/MS. This process revealed another putative intermediate, 3-oxo-19-hydroxy-CL (compound 7) (Fig. 1A and figs. S2 and S20 and table S7). LC-QTOF-MS analysis showed that the accurate mass of compound 7 is consistent with its putative structure (fig. S20). On the basis of these data, we included compound 7 as an intermediate in the postulated steps required to convert CL to zealactol (Fig. 4C and fig. S21).

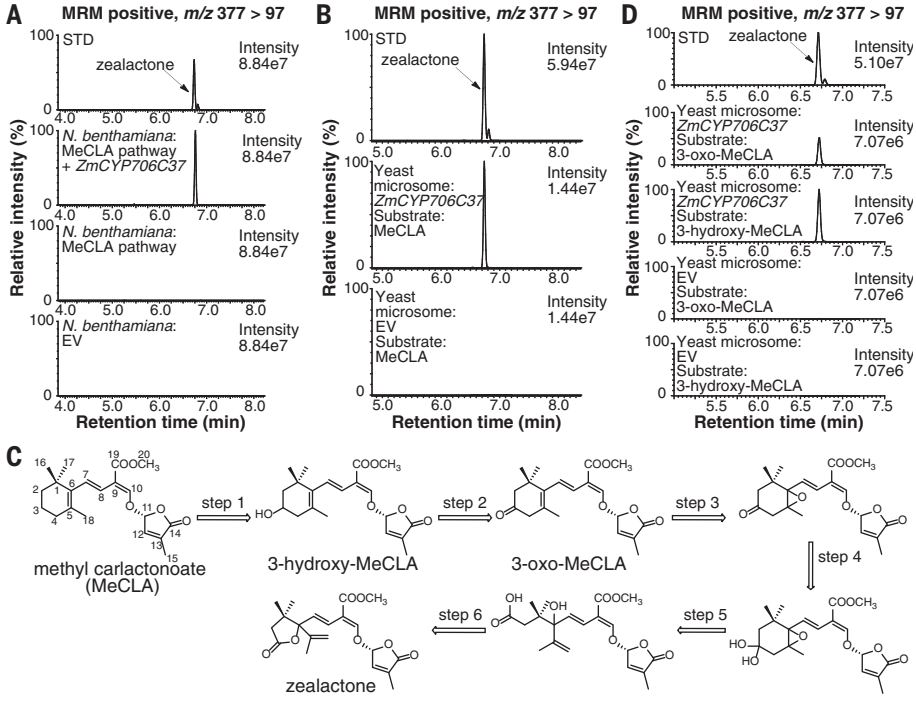


**Fig. 3. Zealactone biosynthesis.** (**A**) Representative MRM–LC/MS/MS chromatograms of zealactone, $[M+H]^+m/z$ 377 > 97, in *N. benthamiana* leaf samples. (**B** and **D**) Representative MRM–LC/MS/MS chromatograms of zealactone from in vitro assays with yeast microsomes expressing *ZmCYP706C37* or empty vector (EV) with methyl carlactonoate (MeCLA), 3-hydroxy-MeCLA, or 3-oxo-MeCLA as substrate. (**C**) Proposed enzymatic conversion of methyl carlactonoate (MeCLA) to zealactone.

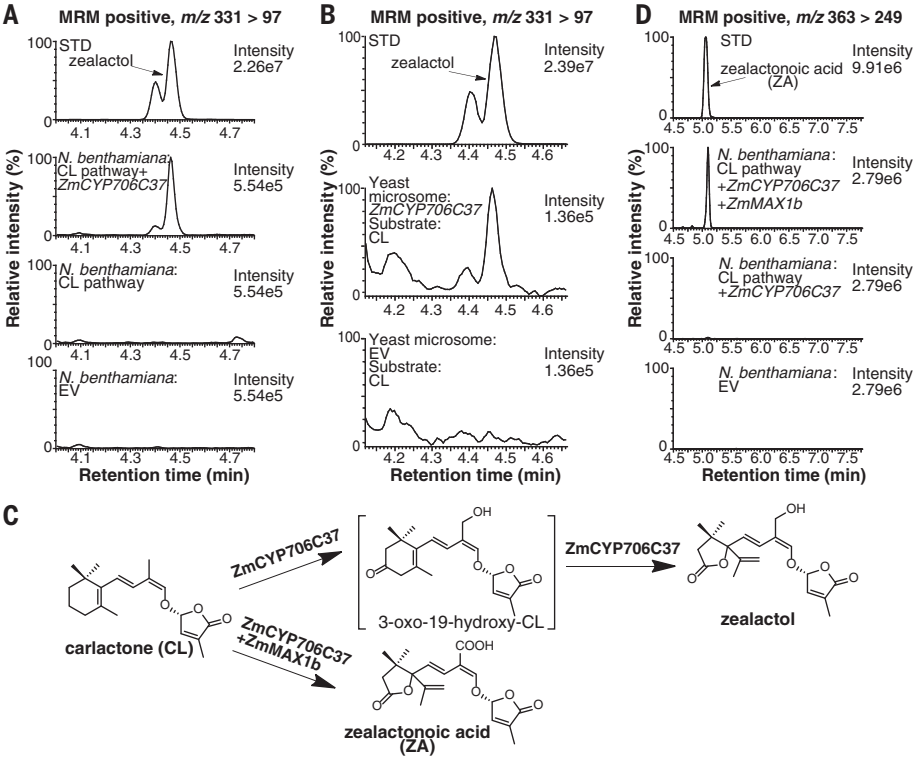


**Fig. 4. Zealactol and zealactonoic acid biosynthesis.** (**A**) Representative MRM–LC/MS/MS chromatograms of zealactol, $[M+H-H_2O]^+m/z$ 331 > 97, in *N. benthamiana* leaf samples. (**B**) Representative MRM–LC/MS/MS chromatograms of zealactol from in vitro assays with yeast microsomes expressing *ZmCYP706C37* or empty vector (EV) with carlactone (CL) as substrate. (**C**) Reactions from CL to zealactol and ZA catalyzed by ZmCYP706C37 and ZmMAX1b. Structure in square brackets is putative. (**D**) Representative MRM–LC/MS/MS chromatograms of ZA, $[M+H]^+m/z$ 363 > 249, in *N. benthamiana* leaf samples. STD, standard; EV, empty vector control. CL pathway, maize carlactone biosynthetic pathway genes, *ZmD27*, *ZmCCD7*, and *ZmCCD8*.

Moreover, agroinfiltration of the CL pathway genes with *ZmCYP706C37* and *ZmMAX1b* resulted in production of ZA, a result also confirmed with LC-QTOF-MS (Fig. 4, C and D, and fig. S22).

Last, analysis of root exudate from a *zmcyp706c37* mutant [EMS4-045ad8, stop-codon gained (fig. S23A)] showed no detectable levels of zealactol, ZA, zealactone, or three other SLs derived from the latter (fig. S23B) (*44*). Although 3-oxo-MeCLA was detectable in the mutant exudate, it was present at a much lower level than in that of the wild type. Instead, CLA and MeCLA accumulated in the mutant exudate, whereas they are absent in the wild type exudate (fig. S23, C and D). Together, these data support our functional characterization of ZmCYP706C37.

### *Biosynthetic control of the maize strigolactone blend*

To determine how the different maize SLs are biosynthetically related, we applied 3-hydroxy-MeCLA, 3-oxo-MeCLA, and zealactol to seedlings

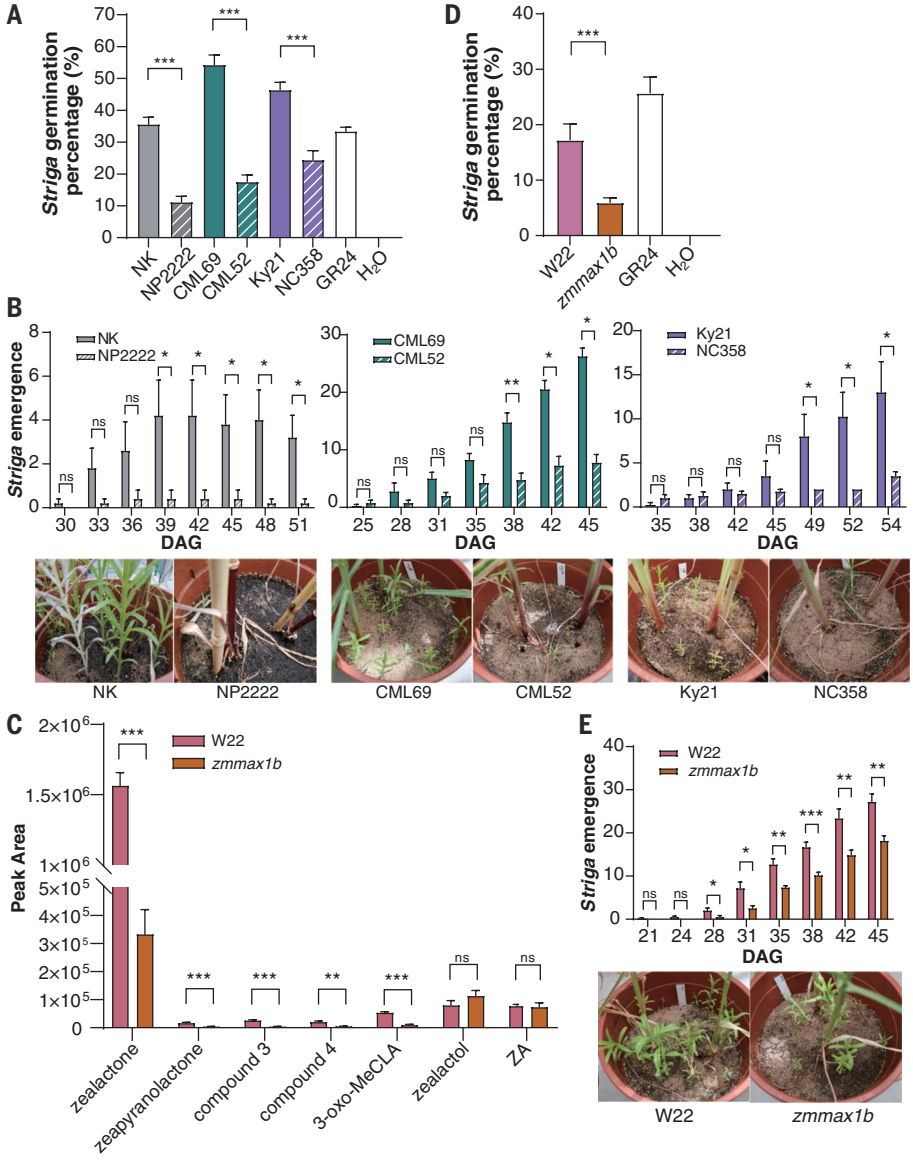


**Fig. 5. Changes in the maize strigolactone blend result in changes in *Striga* resistance.** (**A** and **D**) Induction of *Striga* germination by root exudates of selected maize lines. GR24 (0.335 μM) and water were used as positive and negative control, respectively. (**B** and **E**) *Striga* infection of selected maize lines. Emerged *Striga* numbers were recorded; representative photos highlight the differences. DAG, days after germination of maize. (**C**) SL levels in the root exudate of *zmmax1b* and its wild type, W22. Bars indicate means ± SEM, ns = not significant ($P > 0.05$), *$P < 0.05$, **$P < 0.01$, ***$P < 0.001$, two-tailed, unpaired *t* test.

of another commercial line, NK Falkone, which were treated with fluridone, an inhibitor of SL biosynthesis (*45*). Each of these three compounds complemented zealactone production (fig. S24A), confirming that they can serve as biosynthetic precursors for zealactone. Combined transient expression of *ZmMAX1b* and *ZmCLAMT1* in *N. benthamiana* leaves and subsequent infiltration of zealactol also showed that the latter can be converted to zealactone by ZmMAX1b together with ZmCLAMT1 (Fig. 1A and fig. S25). Application of zealactone to fluridone-treated plants led to the formation of zeapyranolactone and two other maize SLs, designated compounds 3 and 4, suggesting that zealactone is their precursor (Fig. 1A and fig. S24, B to D) (*24*).

Next, we sought mechanisms underlying the distinctive maize SL profile of NP2222 (fig. S26). This line produces zealactone in fluridone-treated seedlings, as does NK Falkone, but only from MeCLA and 3-oxo-MeCLA, not from zealactol (figs. S24A and S26A), suggesting inactivity of MAX1b and/or CLAMT1. As previously noted, ZA accumulated in the root exudate of NP2222 (Fig. 1B and fig. S26D), indicating dysfunction of CLAMT1. Zealactol added to either NK Falkone or NP2222 was converted to ZA, showing that ZmMAX1b is active in NP2222 (fig. S26, B and C). Inspection of the *CLAMT1* sequence in a proprietary NP2222 genome database revealed a large insertion in the second exon of this gene, and reverse transcriptase polymerase chain reaction (RT-PCR) showed that regions flanking the insertion were not transcribed (fig. S26E). These collective data indicate disfunction of CLAMT1 in NP2222.

To analyze biological consequences of the different SL profiles, several maize lines were selected for *Striga* germination and infection assays. The NP2222 root exudate induced much lower germination than that of NK Falkone. Results were consistent with their respective SL profiles and differences in germination-inducing activity of the individual SLs (Figs. 1C and 5A and fig. S26D). CML52 and NC358, both with high proportions of zealactol and ZA, induced significantly less *Striga* germination than did CML69 and Ky21, which produced mostly zealactone despite similar total SL peak areas (Figs. 1C and 5A, and fig. S27, A and B). These differences were also reflected in a *Striga* infection assay with a containerized system, in which *Striga* emergence was less for low-zealactone genotypes (Fig. 5B). In addition to their SL blend, these lines may have other genetic differences that could affect these results. However, we also analyzed a gene-suppression mutant of *ZmMAX1b* (transposon insertion in a W22 background) (fig S28, A and B). This mutant exuded significantly less izealactone and zealactone-derived SLs, whereas the level of zealactol was higher than in the W22 control (Fig. 5C). The *zmmax1b* mutant also induced less *Striga* germination and emergence (Fig. 5E). Results confirm that a change in activity of specific SL biosynthetic enzymes in maize can change the SL composition and confer *Striga* resistance. Although the underlying mechanisms are completely different, these findings resemble those of *lgs* sorghum (*16*) and present a promising prospect for *Striga* resistance breeding in maize. The *zmmax1b* mutant did not exhibit a branching phenotype, in contrast to *zmccd8* (fig. S28C). Also, *zmcyp706c37*, which is located parallel to or downstream of ZmMAX1b, did not display an obvious branching phenotype either. This all suggests that the downstream SLs are not nor precursors of the branching inhibiting hormone and are therefore safe breeding targets that will not result in unwanted pleiotropic effects.

### Conclusions

We have shown that two parallel SL biosynthetic pathways operate in maize and that both pathways produce the major maize SL, zealactone. Changes in flux through these pathways can alter the maize SL profile by shifting the balance between zealactone and zealactol

plus ZA. Zealactol and ZA induce much less *Striga* germination, thus imparting a strong reduction in *Striga* infection to genotypes that exude more zealactol and ZA than zealactone. Future research should investigate whether these changes in the SL blend affect colonization by AM fungi, which was not observed for *lgs* sorghum (*16*). Our results offer a perspective for breeding *Striga* resistance through modification of the SL blend in maize and thus potentially reducing the devastating effects of this parasitic weed in Africa.

## REFERENCES AND NOTES


1. T. Wheeler, J. von Braun, *Science* **341**, 508–513 (2013).
2. B. Badu-Apraku, F. M.A.B., *Advances in Genetic Enhancement of Early and Extra-Early Maize for Sub-Saharan Africa* (Springer Cham, 2017).
3. I. Dörr, *Ann. Bot. (Lond.)* **79**, 463–472 (1997).
4. C. E. Cook, L. P. Whichard, B. Turner, M. E. Wall, G. H. Egley, *Science* **154**, 1189–1190 (1966).
5. A. Besserer *et al*., *PLOS Biol.* **4**, e226 (2006).
6. V. Gomez-Roldan *et al*., *Nature* **455**, 189–194 (2008).
7. S. Al-Babili, H. J. Bouwmeester, *Annu. Rev. Plant Biol.* **66**, 161–186 (2015).
8. M. Umehara *et al*., *Nature* **455**, 195–200 (2008).
9. K. Akiyama, K. Matsuzaki, H. Hayashi, *Nature* **435**, 824–827 (2005).
10. H. Bouwmeester, C. Li, B. Thiombiano, M. Rahimi, L. Dong, *Plant Physiol.* **185**, 1292–1308 (2021).
11. K. Yoneyama *et al*., *J. Exp. Bot.* **69**, 2231–2239 (2018).
12. K. Mashiguchi, Y. Seto, S. Yamaguchi, *Plant J.* **105**, 335–350 (2021).
13. K. Akiyama, S. Ogasawara, S. Ito, H. Hayashi, *Plant Cell Physiol.* **51**, 1104–1117 (2010).
14. N. Mori, K. Nishiuma, T. Sugiyama, H. Hayashi, K. Akiyama, *Phytochemistry* **130**, 90–98 (2016).
15. H. I. Kim *et al*., *J. Pestic. Sci.* **35**, 344–347 (2010).
16. D. Gobena *et al*., *Proc. Natl. Acad. Sci. U.S.A.* **114**, 4471–4476 (2017).
17. A. Alder *et al*., *Science* **335**, 1348–1351 (2012).
18. K. Yoneyama *et al*., *New Phytol.* **218**, 1522–1533 (2018).
19. S. Abe *et al*., *Proc. Natl. Acad. Sci. U.S.A.* **111**, 18084–18089 (2014).
20. C. Cardoso *et al*., *Proc. Natl. Acad. Sci. U.S.A.* **111**, 2379–2384 (2014).
21. Y. Zhang *et al*., *Nat. Chem. Biol.* **10**, 1028–1033 (2014).
22. T. Wakabayashi *et al*., *Sci. Adv.* **5**, eaax9067 (2019).
23. T. Wakabayashi *et al*., *Planta* **251**, 97 (2020).
24. T. V. Charnikhova *et al*., *Phytochemistry* **137**, 123–131 (2017).
25. T. V. Charnikhova *et al*., *Phytochem. Lett.* **24**, 172–178 (2018).
26. X. Xie *et al*., *J. Pestic. Sci.* **42**, 58–61 (2017).
27. M. Yoshimura *et al*., *Helv. Chim. Acta* **103**, e2000017 (2020).
28. M. C. Dieckmann, P.-Y. Dakas, A. De Mesmaeker, *J. Org. Chem.* **83**, 125–135 (2018).
29. T. Kumagai *et al*., *Heterocycles* **36**, 1729–1734 (1993).
30. J. C. Guan *et al*., *Plant Physiol.* **160**, 1303–1317 (2012).
31. K. C. Snowden *et al*., *Plant Cell* **17**, 746–759 (2005).
32. W. Kohlen *et al*., *New Phytol.* **196**, 535–547 (2012).
33. Y. Zhang *et al*., *New Phytol.* **219**, 297–309 (2018).
34. E. Poretsky, A. Huffaker, *PeerJ* **8**, e10264 (2020).
35. S. Stelpflug *et al*, *The Plant Genome* **9**, plantgenome2015.04.0025 (2016).
36. L. Dong *et al*., *Metab. Eng.* **20**, 198–211 (2013).
37. X. Xu *et al*., *J. Exp. Bot.* **72**, 5462–5477 (2021).
38. S. Ma, Z. Ding, P. Li, *BMC Plant Biol.* **17**, 131 (2017).
39. W. J. Kent *et al*., *Genome Res.* **12**, 996–1006 (2002).
40. T. Wakabayashi *et al*., *Planta* **254**, 88 (2021).
41. K. Mashiguchi *et al*., *Proc. Natl. Acad. Sci. U.S.A.* **119**, e2111565119 (2022).
42. Y. Li, K. Wei, *BMC Plant Biol.* **20**, 93 (2020).
43. M. Yoshimura *et al*., *Helv. Chim. Acta* **102**, e1900211 (2019).
44. X. Lu *et al*., *Mol. Plant* **11**, 496–504 (2018).
45. J. A. López-Ráez *et al*., *New Phytol.* **178**, 863–874 (2008).


## ACKNOWLEDGMENTS

We acknowledge S. Al Babili from King Abdullah University of Science and Technology and D. Werck-Reichhart from the University of Strasbourg for helpful discussions, as well as L. Hagmann from Syngenta for his support in NMR analyses and interpretation. **Funding:** This work was funded by the China Scholarship Council (CSC) PhD scholarship 201706300041 (C.L.), the European Research Council (ERC) Advanced grant CHEMCOMRHIZO 670211 (H.J.B.), the Dutch Research Council (NWO/OCW) Gravitation program Harnessing the second genome of plants (MiCRop) 024.004.014 (H.J.B.), the Marie Curie fellowship NEMHATCH 793795 (L.D.). K.E.K and J.G. acknowledge funding from the US National Science Foundation (NSF) Plant Genome Research Program (PGRP) (1421100 and 1748105). **Author contributions:** C.L., L.D., and H.J.B. conceived and designed the project. C.L. discovered and characterized the candidate genes, grew the plants, collected and analyzed the root exudate, cloned the genes, performed agroinfiltration, yeast microsome assay and plant compound treatment assays, and coordinated the project; K.F., T.V.C. and A.C. developed LC-MS methods and helped with SL analysis; T.V.C., J.D., and A.D.J.V.D. helped to establish the biosynthesis mechanisms; J.G. and K.E.K. developed and provided maize seeds (NAM, *zmccd8*, *zmmax1azmmax1c*, and *zmmax1b*) and analyzed RNA-seq and related data. B.T. and L.D. supported the metabolomics analysis; M.Y., K.G., A.D.M. synthesized zealactol and provided zealactone, 3-hydroxy-MeCLA, and 3-oxo-MeCLA; P.Q., R.H., and A.D.M. synthesized zealactonoic acid; J.L., Y.B.S., J.Q., and J.W. grew the *zmcyp706c37* EMS mutants, performed genotyping, selfing, and root exudate collection; H.D.G. collected and prepared the maps of maize and *Striga* occurrence. Y.W. helped with the agroinfiltration and yeast microsome assays; C.L., A.W., and B.T. performed the *Striga* germination and infection bioassays; S.M.C.d.L. and M.H.M. carried out the gene cluster analysis; Y.D. and E.A.S. provided support on coexpression analysis; D.K., K.H. and C.S. provided all commercial maize seeds from Syngenta and coordinated the collaboration with Syngenta. A.M. provided African inbred maize lines. C.L., L.D., and H.J.B. wrote the manuscript, with contributions from other authors. **Competing interests:** M.H.M. is a consultant to Corteva Agriscience, but that company was not involved in this work. All the other authors declare that they have no competing interests. **Data and materials availability:** The maize mutants *zmccd8* and *zmmax1azmmax1c* were obtained via a material transfer agreement (MTA) with the University of Florida Board of Trustees. The RNA-seq data of *zmccd8* and B73 root tissues are available in the NCBI database (BioProject PRJNA757767) under accession numbers of SRR15613590, SRR15613591, SRR15613599, SRR15613593, SRR15613594, and SRR15613595. All the other data are presented in the main text and in the Supplementary Materials. 

## SUPPLEMENTARY MATERIALS

science.org/doi/10.1126/science.abq4775
Materials and Methods
Figs. S1 to S28
Tables S1 to S8
References (*46*–*70*)

View/request a protocol for this paper from *Bio-protocol*.

Submitted 12 April 2022; accepted 30 November 2022
10.1126/science.abq4775